First-principles calculations of the structural and electronic properties of clean GaN (0001) surfaces

A. L. Rosa*
Department of Physics, Uppsala University, Box 530, 75121 Uppsala, Sweden

J. Neugebauer
Max-Planck-Institut für Eisenforschung, Max-Planck-Strasse 1, 40237 Düsseldorf, Germany
(Received 17 August 2005; revised manuscript received 26 January 2006; published 25 May 2006)

We employ density-functional theory (DFT) within the local-density approximation (LDA) and generalized-gradient approximation (GGA) to study structural and electronic properties of clean GaN (0001) surfaces. The pseudopotential method is used to investigate surfaces with (1×1), (2×2), and $(\sqrt{3}\times\sqrt{3})R30°$ reconstructions. We also report calculations for the N_2 molecule and for the bulk phases of Ga and GaN. We find that GGA give better results than LDA for the cohesive energies, but not for the structural properties. Bulk band structures are found to be very similar for both exchange-correlation potentials. Examining the clean GaN (0001) surfaces we conclude that both potentials give very similar relaxations and an almost identical dispersion for the surface states. We also report results for ionization energies, electron affinities, and work function for the GaN (0001) surfaces. As a general trend the ionization energy decreases monotonically with the increasing of the Ga-coverage.

DOI: 10.1103/PhysRevB.73.205346 PACS number(s): 73.20.At, 71.15.Mb

I. INTRODUCTION

The group-III nitrides have attracted much attention in the past years due to their potential application in optoelectronic devices which can operate from the infra-red to ultra-violet regions of the spectrum.[1–3] GaN has been by far the most intensively studied material among the group-III nitrides. The structural and electronic properties of GaN surfaces depend sensitively on the orientation of the surface, surface termination, and reconstruction.[4–8] The most common growth direction of epitaxial hexagonal GaN is normal to the {0001} basal plane (see, for example, Ref. 9 and references therein). It is important to note that the (0001)(or Ga-polar) and $(000\bar{1})$(or N-polar) directions are not equivalent and exhibits different properties.

The GaN (0001) surfaces have been demonstrated to have a better surface morphology and are therefore the relevant surfaces for technological applications.[3] Depending on the growth conditions the GaN (0001) surface exhibits a large variety of reconstructions, such as (1×1), (2×2), (4×4), (5×5), and (6×4).[10–14]

Several theoretical and experimental studies were devoted to identifying the electronic structure of these surfaces. The (2×2) reconstruction has been explained as being a N-adatom structure under N-rich conditions and a Ga-adatom structure under Ga-rich conditions.[12] The (5×5) structure has been proposed to consist of Ga and N adatoms[12] and for the (4×4) and (6×4) the atomic structure has not been completely clarified yet. Particular attention has been given to the (1×1) structure, which is observed at extreme Ga-rich conditions. This structure has been identified as a Ga bilayer termination, with Ga coverage between 2 and 3 ML (monolayers).[4,11] Theoretical support is given by first-principles calculations which suggested that the best candidate for this structure is a laterally contracted Ga-bilayer structure with approximately 2.3 ML of Ga.[15]

Concerning the atomic structure, Sung *et al.*[16] concluded from their low energy electron diffraction (LEED) studies that both GaN (0001) and $(000\bar{1})$ surfaces are neither reconstructed nor relaxed. Yu *et al.*[17] used quantitative LEED and concluded that the best fit structural model for a series of (1×1) structures was a Ga adlayer on the top of a Ga terminated surface.

The electronic structure of (1×1) surfaces of GaN films grown by molecular beam epitaxy (MBE) was addressed by angle-resolved photoemission spectroscopy (ARPES) by Dhesi *et al.*[18] In addition to the bulk bands, they observed a dispersionless surface state band near the valence band maximum.

Chao *et al.*[19] reported a more complete account on the electronic structure of the (1×1) surfaces using synchrotron-radiation-excited ARPES. However, as ARPES does not provide unambiguous information about the termination or polarity of the films, the observed states can be due either from the (0001) or $(000\bar{1})$ surface. One band, close to the valence band maximum, was found to be weakly dispersive and very sensitive to the hydrogen adsorption, suggesting the surface has dangling bonds at the outermost layer. The other band was found to be very sensitive to the quality of the sample, as determined by LEED.

Recently Widstrand *et al.*[20] have used angle-resolved ultraviolet photoelectron spectroscopy (ARUPS) to study Ga-polar GaN (0001) surfaces. They identified one surface state close to the top of the valence band at the Γ point dispersing down and emerging into the projected band gap around the K point.

Wang *et al.*[21] performed density-functional theory calculations within the local-density approximation using pseudopotential method for the clean (0001) and $(000\bar{1})$ surface in

order to compare with the available experimental data. By calculating the atomic and electronic structure of several possible (1×1) structures, they concluded that the clean Ga-terminated surface has a very small relaxation. Concerning the electronic structure, none of the Ga-polar structures was consistent with the ARPES data by Chao *et al.*[19] Instead, the best agreement with the experimental result was achieved when comparing the theoretical surface states of the N-terminated $(000\bar{1})$ surface.

Recently Timon *et al.*[22] reported adsorption of N and Ga layers on the top of bare Ga-terminated (2×2) GaN (0001) surfaces. They concluded that the N-adatom structure is energetically more stable under N-rich conditions while the Ga adlayer is more favorable under Ga-rich conditions.

Other important surface properties are the work function, ionization energy (or photoelectric threshold), and electron affinity. Those quantities are relatively easy to measure and allow us to monitor changes in the surface geometry. However, few experiments are available and are not conclusive. For example, values for the electron affinity of GaN surfaces lie in the range of 2.6–3.5 eV.[23–26] First-principles calculations have been performed by Grossner *et al.*[27] for the (111) face of the GaN in cubic phase.[27] However, to the best of our knowledge, no calculation has been performed for the GaN (0001) surfaces.

In this work we will therefore focus on the study of the structural and electronic structure of the most relevant clean GaN (0001) surfaces employing density-functional theory within the local-density approximation. The use of generalized gradient approximation for treating these surfaces is also discussed. First-principles calculations for the ionization energy, electron affinity, and work function of various clean (0001) GaN surfaces are presented.

This paper is divided as follows. In Sec. II we give a brief description of the computational details. Then in Sec. III we discuss our results for the bulk properties of GaN-bulk, Ga-bulk, N_2 molecule making a comparison between local-density approximation (LDA) and generalized-gradient approximation (GGA). Then we present our results for the clean GaN (0001) surfaces and discuss the role of the exchange-correlation potential. Also, calculations for ionizatoion energy, work function, and electron affinity are discussed. Section IV contains our conclusions.

II. COMPUTATIONAL DETAILS

In this work we employ density-functional theory[28,29] in the LDA[30] as parametrized by Perdew-Zunger[31] and GGA as parametrized by Perdew, Burke, and Ernzerhof (PBE)[32] to study the GaN (0001) surfaces. We use norm-conserving, nonlocal pseudopotentials generated within the Troullier-Martins scheme.[33,34]

For Ga we use the configuration $3d^{10}4p^24p^1$ and the cut-off radii $r_s=2.08$ bohr, $r_p=2.30$ bohr, and $r_d=2.08$ bohr, treating the s as local component to avoid ghost states. For N we use the configuration $2s^22p^23d^0$ with the following cut-off radii: $r_s=1.5$ bohr, $r_p=1.5$ bohr, and $r_d=1.5$ bohr, and the s component as the local component. Those pseudopotentials have been successfully used to describe bulk properties GaN.[42,43] The electron wave functions are expanded in a plane wave basis set using a 70 Ry cut-off energy. We use the Monkhorst-Pack scheme[35] to generate the special **k** points in the irreducible part of the Brillouin zone (IBZ). For cubic GaN we use a $(6\times6\times6)$ mesh, for hexagonal GaN a $(6\times6\times3)$ mesh, and for α-Ga a $(8\times8\times8)$ mesh. For the N and Ga atoms and N_2 molecule calculations we have used a cubic cell with side $L=10$ Å and the special **k** point $(1/4,1/4,1/4)$. The surfaces are treated using periodically repeated slabs with eight (nine) layers of GaN to model the clean N (Ga)-terminated surface. For the monolayer and bilayer structures one or two additional layers of Ga were considered. We have used a vacuum region of 11 Å throughout the surface calculations. One side of the slab is saturated with pseudohydrogen atoms of fractional charge $0.75e^-$ to recover a bulklike behavior. The surface unit cells with (1×1), $(\sqrt{3}\times\sqrt{3})$, and (2×2) periodicity we used meshes with $(4\times4\times1)$, $(3\times3\times1)$, and $(2\times2\times1)$ **k** points, respectively.

The cohesive energies of GaN bulk, Ga bulk, and N_2 molecule (Tables I–IV) are calculated from the ground-state total energies of the crystals $E_{\mathrm{tot}}^{\mathrm{bulk}}$ and the free atoms E_{atom_i} as follows:

TABLE I. Calculated structural and thermodynamic properties of Ga bulk in the α phase using LDA and PBE: equilibrium lattice parameters a_0, b_0/a_0, c_0/a_0, u and v and cohesive energy E_{coh}. The experimental lattice parameters were taken from Refs. 41 and 66. In our calculations they were not optimized. Parameters used in the calculations: 70 Ry energy cutoff and 216 **k** points in the IBZ. The cohesive energy was corrected by a spin-polarization correction of 0.145 eV (LDA) and 0.179 eV (PBE). These values were extracted from Ref. 43. A comparison with experimental data is also provided.

	a_0 (Å)	b_0/a_0	c_0/a_0	u	v	E_{coh} (eV)
LDA	4.51	1.001	1.695	0.0785	0.1525	−3.29
PBE	4.51	1.001	1.695	0.0785	0.1525	−2.54
Exp.[a]	4.511	1.001	1.695	0.0785	0.1525	−2.81

[a]Reference 41.

TABLE II. Calculated bond length d, binding energy E_b, and vibration frequency ω for a N_2 molecule using LDA and PBE. Our binding energy values were corrected by a spin-polarization correction of 3.03 eV (LDA) and 3.12 eV (PBE). These values were extracted from Ref. 42. We use a cubic supercell with length $L=10$ Å, 1 **k** point $(1/4,1/4,1/4)$ in the IBZ, and 70 Ry cut-off energy. The zero point vibration energy (ZPE) of the molecule was included in our calculations. The experimental values are also given.

	d (Å)	E_b (eV)	ω (cm^{-1})	ZPE (eV)
LDA	1.09	−11.71	2363	0.146
PBE	1.09	−10.66	2331	0.153
Exp.[a]	1.10	−9.82	2360	

[a]Reference 67.

TABLE III. Calculated structural and thermodynamic properties of β GaN using LDA and PBE: equilibrium lattice constant a_0, bulk modulus B_0, bulk modulus derivative B_0', cohesive energy E_{coh}, and formation enthalpy $\Delta H_f^{\mathrm{T=0}}$. An energy cutoff of 70 Ry and 28 **k** points in the IBZ were used. The cohesive energy was corrected by a spin-polarization correction of 0.145 eV (LDA) and 0.179 eV (PBE) for the Ga atom and 3.03 eV (LDA) and 3.12 eV (PBE) for the N atom. Experimental values for those properties are also given.

	a_0 (Å)	B_0 (Mbar)	B_0'	E_{coh} (eV)	$\Delta H_f^{\mathrm{T=0}}$ (eV)
LDA	4.52	1.88	4.35	−10.38	−1.22
PBE	4.60	1.66	4.12	−8.52	−0.62
Exp.[a]	4.52	1.73	3.70	−8.96	−1.20

[a]References 48 and 68.

$$E_{\mathrm{coh}} = E_{\mathrm{tot}}^{\mathrm{bulk}} - \sum_i E_{\mathrm{tot}}^{\mathrm{atom_i}}. \quad (1)$$

One should note that in order to calculate the total energy of a free atom using periodic boundary conditions, some technical aspects should be considered. A large cubic supercell is needed to prevent that one atom from a certain unit cell interacts with an atom of a neighboring unit cell. In the calculation of the cohesive energy we include the so-called spin-polarization correction energy for the spin-saturated spherical free- (pseudo-) atom by adding the difference of the total energies of the spin-polarized and saturated all-electron atom within the respective exchange-correlation scheme.

The formation enthalpy for GaN bulk $\Delta H_f^{\mathrm{T=0}}$ (Tables III and IV) is calculated as

$$\Delta H_f^{\mathrm{T=0}} = E_{\mathrm{tot}}^{\mathrm{GaN\ bulk}} - E_{\mathrm{tot}}^{\mathrm{N_2\ molecule}} - E_{\mathrm{tot}}^{\mathrm{Ga\ bulk}}, \quad (2)$$

where $E_{\mathrm{tot}}^{\mathrm{GaN\ bulk}}$, $E_{\mathrm{tot}}^{\mathrm{N_2\ molecule}}$, $E_{\mathrm{tot}}^{\mathrm{Ga\ bulk}}$ are the total energies of GaN bulk, N_2 molecule, and Ga bulk, respectively.

III. RESULTS

Before starting surface calculations for any material, it is crucial to perform calculations for its bulk phase in order to determine the structural and thermodynamic properties. In particular, the lattice parameters of the bulk phase will be needed to perform the calculations of surfaces. Also, in the approach we use, the formation enthalpy is a quantity necessary to calculate the surface energies. It is therefore assumed that the calculated properties are transferable and the properties determined using smaller systems like the bulk phase hold also for surfaces.

TABLE IV. Calculated structural and thermodynamic properties of α-GaN using LDA and PBE: equilibrium lattice constants a_0, c_0/a_0 ratio, internal parameter u, bulk modulus B_0, bulk modulus derivative B_0', cohesive energy E_{coh}, and formation enthalpy $\Delta H_f^{\mathrm{T=0}}$. An energy cutoff of 70 Ry and 33 **k** points in the IBZ were used. The cohesive energy was corrected by a spin-polarization correction of 0.145 eV (LDA) and 0.179 eV (PBE) for the Ga atom and 3.03 eV (LDA) and 3.12 eV (PBE) for the N atom. Experimental values for those properties are also given.

	a_0 (Å)	c_0/a_0	u	B_0 (Mbar)	B_0'	E_{coh} (eV)	$\Delta H_f^{\mathrm{T=0}}$ (eV)
LDA	3.196	1.631	0.375	1.87	5.39	−10.40	−1.25
PBE	3.252	1.629	0.376	1.62	4.06	−8.54	−0.64
Exp.[a]	3.189	1.624	0.375	1.88	4.3	−9.06	−1.15

[a]Reference 48.

A. Ga bulk

Ga bulk has different bulk phases [Ga-II, Ga-III,[36] α,[37] β,[38] γ,[39] δ,[40] and ϵ (Ref. 36)], depending on the pressure and temperature. Several theoretical and experimental studies have shown that α-Ga is the stable phase at room temperature and low pressure (up to 16×10^3 atm).[41] Here we concentrate on the properties of α-Ga only. The α phase has an orthorhombic structure with eight atoms per unit cell which have the atomic positions $(\pm u, 0, \pm v)$, $(1/2\pm u, 0, 1/2\pm v)$, where u and v are the internal parameters.

A peculiar feature is that each atom has only one nearest neighbor at a distance of 2.44 Å. The second, third, and fourth shell each contain two atoms and are 0.27, 0.30, and 0.39 Å further away. For the sake of computational effort, all properties were calculated at the experimental geometry, i.e., the structure was not relaxed.

The results for the calculated and experimental properties are shown in Table I. The cohesive energy is overestimated by around 15% using LDA, while for PBE it is underestimated by 10%. Comparing our results with the ones of Ref. 42, where the structure was fully optimized using the full potential linear augmented plane wave (FP-LAPW) method, the difference in the lattice parameters is less than 0.1 Å and in the cohesive energy less than 0.2 eV.

B. N_2 molecule

The total energy calculations for a N_2 molecule in gas phase were carried out using a cubic cell of 10 Å, which was found to be large enough to avoid interaction with other molecules in the neighboring cells. The results for the binding energy, bond length, and vibration frequency for the N_2 molecule are shown in Table II. The vibration frequency is calculated using a third-order polynomial fit to the total energy versus N_2 bond length curve. The present results are in good agreement with previous LDA and PBE calculations using the pseudopotential approach.[42] Compared to the LDA results, PBE gives slightly longer bond lengths, lower frequencies, and smaller binding energies, i.e., PBE values are closer to experiment. The binding energy is overestimated by 16% using LDA and 8% using PBE.

C. Wurtzite and zinc-blende GaN

1. Atomic and thermodynamic properties

GaN crystallizes preferentially in the wurtzite structure. Stabilization of the zinc-blende structure has been reported for growth (001) faces of cubic materials, such as GaAs, SiC and Si.[44] The zinc-blende and wurtzite structures are sche-

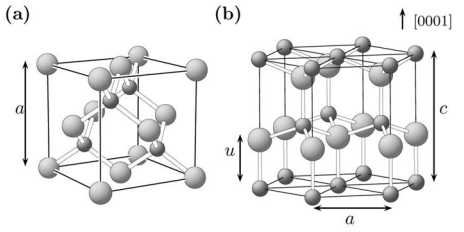

FIG. 1. Conventional unit cells of (a) β-GaN (zinc-blende structure) and (b) α-GaN (wurtzite structure). a and c are the lattice parameters and u is the internal parameter. Ga atoms are denoted by big gray circles and N atoms by small gray circles.

matically shown in Figs. 1(a) and 1(b). The zinc-blende structure has two atoms (1 Ga and 1 N) per unit cell at the positions (0,0,0) and (1/4,1/4,1/4) and the wurtzite structure has four atoms (2 Ga and 2 N) per unit cell at the positions (0,0,0), (2/3,1/3,1/2), (0,0,u), and $(2/3, 1/3, u+1/2)$.

The equilibrium structure for GaN bulk is obtained by minimization of the total energy with respect to the primitive unit cell volume V. In the zinc-blende structure the volume is directly related to the lattice constant a ($V=a^3/4$), while for the wurtzite structure the volume is a function of the lattice parameters c and a ($V=\sqrt{3}a^2c/2$). Therefore, for the wurtzite structure, the minimization has to be performed by a two-step procedure: The ratio c/a and the internal parameter u have to be optimized for each given volume V. This procedure is repeated for other volumes near the experimental one. We chose for all cases a range from −9 to +9 % around the experimental value. Fitting these values to the Murnaghan equation of state we have obtained the values for the equilibrium lattice constant, bulk modulus, and bulk modulus derivative.

The total energy differences per Ga-N pair for GaN bulk versus the normalized volume V/V_0 (V_0 is the experimental volume) are presented in Fig. 2. We find that this difference is 16 meV/pair. This difference is in good agreement with

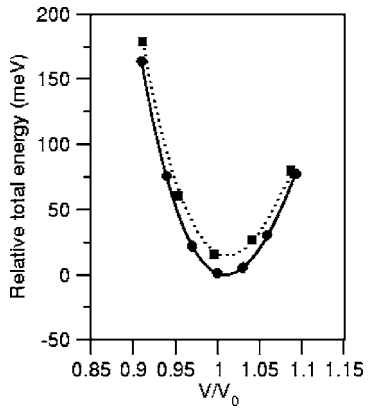

FIG. 2. Calculated total energy difference of GaN bulk per Ga-N pair versus normalized volume V/V_0 using LDA. V_0 is the experimental volume for GaN in the wurtzite structure. The solid line refers to the hexagonal phase (wurtzite structure), while the dotted line refers to the cubic phase (zinc-blende structure). The energy reference is set on the lowest energy value for the wurtzite structure.

other theoretical results,[45–47] where it was found that the difference in energy between the two structures less than 20 meV. Our results also agree with experiment, where the hexagonal phase of GaN is found to be the most stable phase.[48]

The discussion of the lattice parameters of GaN concerns both cubic and hexagonal phases, otherwise noted. Tables III and IV show the results for the calculated bulk properties: lattice constants a_0 and c_0/a_0, bulk modulus B_0, first derivative of the bulk modulus B_0', cohesive energy E_{coh}, and formation enthalpy $\Delta H_f^{\mathrm{T=0}}$.

We find that the LDA lattice parameters (for the cubic and hexagonal phases) are smaller than the experimental ones by around 1%. The cohesive energy using LDA is overestimated with respect to the experimental value by 17% and the formation enthalpy by 8%. The lattice parameter with PBE overcorrects and gives a 1.7% (1.9%) too large value for the zinc-blende (wurtzite) structure compared to experiment.

The GaN cohesive energy is overestimated by 6% compared to the experimental result, which confirms the fact that PBE improves the binding energies in many solids.[49–52] However, the formation enthalpy (−0.64 eV) is underestimated by 44% compared to the experimental value (−1.15 eV).

In order to understand this behavior, the individual contributions (N_2 molecule, Ga bulk, and GaN bulk) to calculate the formation enthalpy are analyzed. The formation enthalpy involves the binding energies of solid phases of the constituent systems. From our results, we find that LDA always overestimates the cohesive energy for the constituent species with respect to the experimental value, which means that the error is always positive. For the N_2 molecule this error is +0.94 eV, for α-Ga +0.48 eV and for GaN-bulk +0.67 eV. Thus the difference among the individual terms brings the LDA value close to the experimental one.

However, for PBE, the error for the individual systems have different signs: For the N_2 molecule the error is positive (+0.42 eV), whereas for the GaN bulk (−0.27 eV) and Ga bulk (−0.26 eV) the error is negative. Therefore, the difference pushes the PBE value far from the experiment. Based on the results discussed above, we can draw the following conclusions: (i) the magnitude of the error of the structural properties are similar using LDA and PBE; however, in different directions: LDA underestimates the lattice parameters whereas PBE underestimates them; (ii) PBE gives better results than LDA for the structural properties and cohesive energy of all compounds (Ga bulk, N_2 molecule, and GaN bulk); (iii) PBE performs worse than LDA for the formation enthalpy, but we can explain it noticing that the description of the binding energies for the N_2 molecule and the bulk phases have errors with different signs with respect to the experimental value.

Compared to all-electron calculations, PP-LDA gives an error of 0.3 eV. Ultra-soft pseudopotential[53] results overestimate the formation enthalpy by 0.5 eV when LDA is used, but are in very close agreement when PBE is used (difference of 0.1 eV).

2. Electronic properties

Figures 3(a)–3(d) show our results for the band structure calculations of GaN in the wurtzite and zinc-blende struc-

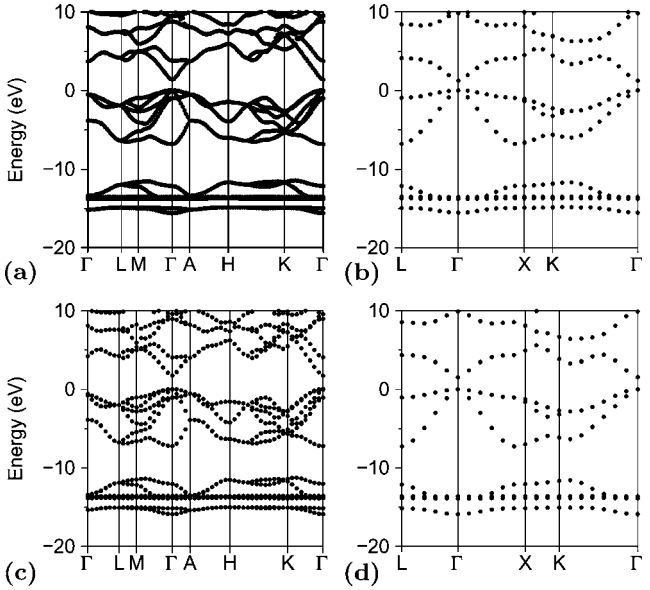

FIG. 3. Bulk band structure of hexagonal (wurtzite) and cubic (zinc-blende) GaN. (a) Hexagonal phase using PBE, (b) cubic phase using PBE, (c) hexagonal phase using LDA, and (d) cubic phase using LDA. The optimized theoretical lattice constants were used for the calculations.

tures using LDA [(c) and (d)] and PBE [(a) and (b)]. The band structure was calculated at the optimized geometry for both structures. Both phases have a direct band gap, with valence band maximum and conduction band minimum located at the Γ point of the Brillouin zone.

While there is a single conduction band with Γ_7 symmetry, there are three valence bands, which are nondegenerate. Due to the spin-orbit and crystal field splitting, the top of the valence band separates in three bands, two with Γ_7 symmetry (light-hole and spin-orbit splitting band) and one with Γ_8 symmetry (heavy hole). In this calculation, we do not include spin-orbit coupling. However, the splitting due to the crystal-field is found to be 10 meV. The experimental values lie in the range of 10–25 meV.[48]

We can see that the band structures look almost identical for both exchange-correlation functionals. As expected, LDA and GGA severely underestimate the band gap. For the cubic phase we find a band gap of 1.60 eV using LDA, while using PBE we find 1.27 eV. For the hexagonal phase, we find a gap of 1.76 eV using LDA whereas using PBE we found 1.39 eV.

D. The GaN (0001) surface

1. Surface reconstructions and relaxations

In the present work, the unreconstructed Ga and N-terminated (0001) surfaces are modeled using an (1×1) surface unit cell. A top view of these surfaces is shown in Fig. 4(a). A side view of these surfaces is shown in Fig. 4(b) (N terminated) and Fig. 4(c) (Ga terminated). Each (1×1) unit cell contains one atom per layer. Structures with a Ga adatom and N adatom are modeled using a (2×2) unit cell. Each (2×2) cell contains four atoms in each of the underlying layers and one additional atom per layer. A top view of the (2×2) unit cell is shown in Fig. 4(a) and a side view is shown in Figs. 4(d) and 4(e). There are many possible sites to adsorb atoms on the surface. Here we consider the highest symmetry adsorption sites, *hcp, fcc*, and *ontop*, as shown in Fig. 4(a).

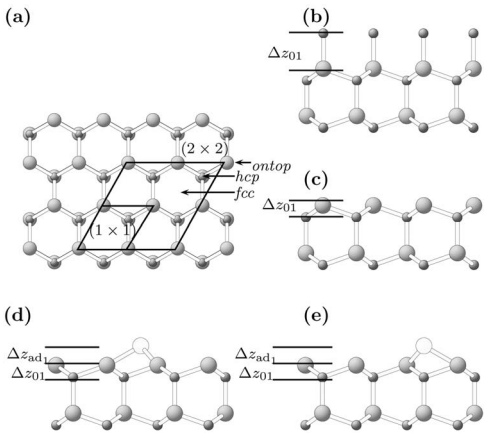

FIG. 4. (a) Top view of the (1×1) and (2×2) unit cells used to model the GaN (0001) surfaces. The highest symmetry sites *fcc, hcp*, and *ontop* are indicated. (b) Side view of the clean N terminated, (c) clean Ga-terminated, (d) adatom-*fcc* structure, and (e) adatom-*hcp* structures. *d* is the bond length between the adatom (Ga or N) to the Ga atoms at the first plane, Δz_{ad_1} is the distance between the adatom and the first plane, and Δz_{01} the distance between the first and second plane. Small gray circles are N atoms, big gray circles mark the Ga atoms, and white circles the (Ga,N) adatoms.

In addition to the clean and adatom structures, we have also studied structures where additional Ga layers lay on the top layer of the clean Ga-terminated surface. The side view of a strucure with an additional Ga layer (Ga adlayer) on the top of the clean Ga-terminated surface is shown in Fig. 5(a) and with two Ga layers (Ga-bilayer) on the top of the clean Ga-terminated surface is shown in Fig. 5(b). Besides, we also studied structures where the outermost top layer was contracted. To model the laterally contracted adlayer and bilayer structures we employ a $(\sqrt{3}\times\sqrt{3})R30°$ unit cell, as has been suggested in Ref. 15.

In these $(\sqrt{3}\times\sqrt{3})R30°$ cells there are four atoms in the laterally contracted hexagonal overlayer for every three atoms in the (1×1) underlying hexagonal layer. The lattice vectors of the overlayer are rotated by 30 deg with respect to those of the substrate. From now on we will call this cell $(\sqrt{3}\times\sqrt{3})$. Such a model allows the Ga-Ga spacing to be close to the value which minimizes the formation energy of a free standing layer of Ga. Consequently, the $(\sqrt{3}\times\sqrt{3})$ cell should provide a very good upper bound for the energy of the optimal laterally contracted overlayer structure.

The laterally contracted Ga-Ga spacing is $a_c=(\sqrt{3}/2)a_{1\times1}=2.75$ Å, where $a_{1\times1}=3.19$ Å is the in-plane spacing of Ga atoms on the (1×1) unit cell, i.e., the Ga adatoms are compressed by around 14% compared to the full monolayer. The side view of the contracted Ga-bilayer structure is shown in Fig. 5(c) and of the contracted Ga-adlayer structure in Fig. 5(d). The top view of the contracted Ga-adlayer and Ga-bilayer structures is shown in Fig. 5(e).

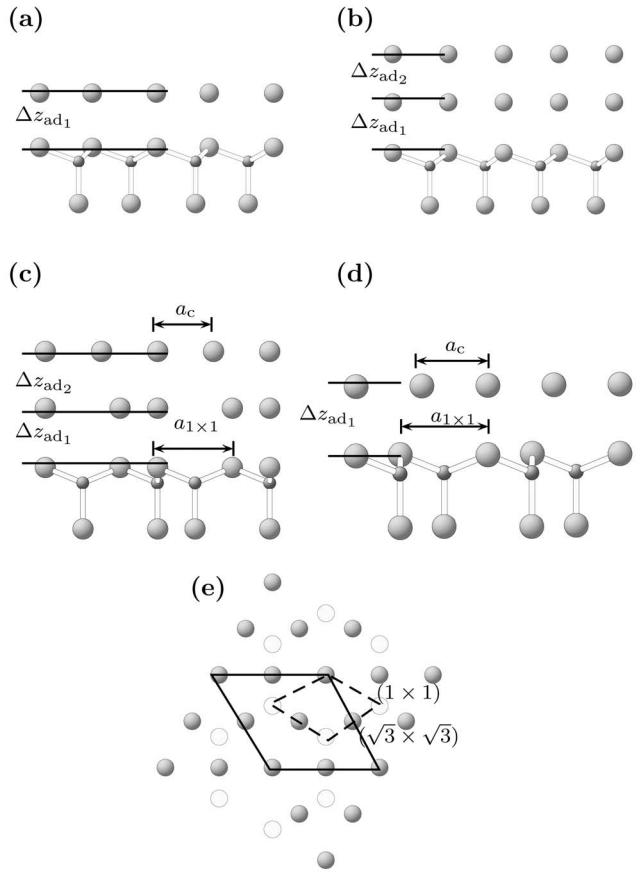

FIG. 5. (a) side view of the Ga-adlayer structure, (b) side view of the Ga-bilayer structure, (c) side view of the contracted Ga-bilayer strucure, and (d) side view of the contracted Ga-adlayer strucure. Δz_{ad_1} and Δz_{ad_2} indicate the distance between the first and second planes and between the second and third planes, respectively. In (c) and (d) the pictures were rotated by 30 deg for ease of viewing. (e) Top view of the contracted Ga-adlayer and Ga-bilayer structures with the top layer [gray circles having a $(\sqrt{3}\times\sqrt{3})$ unit cell] and second layer [white circles having a (1×1) unit cell].

For all of these structures the equilibrium geometry has been calculated. For the unreconstructed (1×1) surfaces the three topmost layers have been allowed to relax. For the adatom structures the two top layers in addition to the adatom were relaxed. For the contracted and noncontracted structures the four outermost layers were allowed to relax. The forces on the atoms are converged up to 5×10^{-3} eV/Å. The noncontracted structures will be considered later on. In Table V we show results for the surface relaxations of the structures described above.

The atomic geometries of GaN (0001) surfaces are quite similarly described by LDA and PBE. The main discrepancy is for the N adatom structure where LDA gives slightly larger values for the interlayer spacing between the adsorbate plane and the first plane. However, the distance d is very similar in both cases. This is because the relative relaxation of the top layers is almost the same using both functionals. The LDA results are in good agreement with previous LDA studies,[54] for the Ga- and N-adatom relaxations.

For the adatom structures, we can see that the hollow sites *fcc* and *hcp* show a different behavior when N is the adatom. For the *fcc* site, the distance between the N adatom and the first plane formed by Ga atoms is much larger than for the *hcp* structure. This stems from the fact that N at the *hcp* site feels the presence of the N atom at the third layer directly below, while for the *fcc* site it does not occur, as pointed out in Refs. 55 and 56. For the Ga adatom, the relaxations for the *fcc* and *hcp* sites are almost identical. For the contracted Ga-bilayer structures the spacing between the Ga atoms between the first and the second layer (2.37 Å) and between the second and the third layer (2.50 Å) are close to that of the nearest neighbor distance in the α-Ga bulk phase (2.44 Å). For the contracted Ga adlayer the distance between the Ga atoms in the first and second layers is 2.47 Å. These results are in very close agreement to the results of Ref. 15. For the noncontracted bilayer, the distance between the Ga atomic layers (first and second planes and second and third planes) are very similar to the contracted Ga bilayer, meaning that the energy gain of the contracted bilayer can be attributed to the reduction of the in-plane spacing.

Our results using PBE are very similar to the results using LDA. For the contracted Ga-bilayer structures the spacing between the Ga atoms in the first and second layers is 2.38 Å and between the second and third layers is 2.58 Å. For the contracted Ga adlayer the distance between the Ga atoms in the first and second layers is 2.49 Å.

Recent experimental results using LEED have concluded that the best fit for the (1×1) Ga-terminated surface consists of an ordered adlayer ontop of a Ga-terminated surface.[17] They found that the spacing between the Ga atoms in the first and second layers is 2.51 Å and between the second and third layers is 0.72 Å. These values are in very good agreement for our contracted Ga adlayer. The contraction itself does not change the adatom spacing significantly, as we can see from Table V.

2. Surface energy

The surface energy is the energy necessary to create two equivalent surfaces by cleaving the crystal along a certain plane. However, for the GaN (0001) surface, it is not possible to calculate the absolute surface energy since it is not possible to build up two equivalent surfaces cleaving the GaN crystal along the {0001} plane. Therefore, what we calculate is the relative surface energy.[10] We have chosen the clean Ga-terminated surface as reference (zero of energy).

In order to compare the stability of the studied structures with a different number of atoms and species, the surface energy is written as follows:[57]

$$E_{\text{surf}}(\mu_N,\mu_{Ga}) = E_{\text{tot}}^{\text{slab}} - \mu_N n_N - \mu_{Ga} n_{Ga} - E_{\text{clean}}, \qquad (3)$$

where $E_{\text{tot}}^{\text{slab}}$ is the total energy of the slab with various reconstructions, μ_α is the atomic chemical potential of Ga and N, n_α is the number of atoms of each specie α and E_{clean} is the energy of the clean Ga-terminated surface. Assuming thermodynamic equilibrium, the N and Ga chemical potentials are not independent, but related by $\mu_{GaN}=\mu_{Ga}+\mu_N$, where μ_{GaN} is the GaN chemical potential. In order to ensure that the surfaces are stable against the formation of undesirable

TABLE V. Calculated relaxations using LDA and PBE for the clean Ga and N terminated, Ga- and N-adatom structures, Ga-adlayer and Ga-bilayer surfaces as defined in Figs. 4(b)–4(e) and 5(a)–5(d) and d is the bond length between the adatom and the surface, Δz_{01} is the distance between the first and second planes for the clean surfaces, Δz_{ad_1} is the distance between the adatom and the first plane for the adatom, Ga-adlayer and Ga-bilayer structures and Δz_{ad_2} is the distance between the second and third planes for the Ga-bilayer structures. All values are given in angstroms.

	Unreconstructed		N adatom		Ga adatom		Ga bilayer		Ga adlayer
	N term	Ga term	*hcp*	*fcc*	*hcp*	*fcc*	Cont.	Noncont	Cont
					LDA				
d			2.05	2.01	2.46	2.47			
Δz_{01}	1.92	0.66	0.62	0.70	0.65	0.80	0.68	0.58	0.68
Δz_{ad_1}			1.13	1.51	1.57	1.57	2.37	2.34	2.47
Δz_{ad_2}							2.50	2.41	
					PBE				
d			2.09	2.05	2.50	2.53			
Δz_{01}	1.97	0.69	0.60	0.91	0.75	0.82	0.67	0.59	0.69
Δz_{ad_1}			0.90	1.15	1.67	1.65	2.38	2.36	2.49
Δz_{ad_2}							2.58	2.44	

phases the following boundary conditions have to be obeyed:

$$\mu_{\mathrm{Ga}} < \mu_{\mathrm{Ga(bulk)}} \quad \text{and} \quad \mu_{\mathrm{N}} < \mu_{\mathrm{N_2(molecule)}}. \tag{4}$$

Using these conditions we obtain that the range of the thermodynamically allowed chemical potential for N and Ga is given by

$$\Delta \mathrm{H}_f^{\mathrm{GaN}} < \mu_{\mathrm{N}} - \mu_{\mathrm{N_2(molecule)}} < 0 \tag{5}$$

and

$$\Delta \mathrm{H}_f^{\mathrm{GaN}} < \mu_{\mathrm{Ga}} - \mu_{\mathrm{Ga(bulk)}} < 0, \tag{6}$$

where $\Delta \mathrm{H}_f^{\mathrm{GaN}}$ is the GaN heat of formation.

It can be shown that the experimentally relevant range of p and T the formation enthalpy changes by less than 0.05 eV.[58] Therefore, the temperature and pressure dependence will be disregarded. If zero point vibrations are neglected the chemical potentials at $p,T=0$ is the internal energy (per number of atoms) of the crystal.

In Figs. 6(a) and 6(b) we show the results for the relative surface energy of the clean Ga- and N-terminated surfaces, Ga and N adatoms at *fcc* and *hcp* positions on the clean Ga-terminated, Ga-adlayer, and Ga-bilayer structures. We compare PBE and LDA in order to verify whether they provide the same sequence in energy of surface energies. Our results for LDA are in excellent agreement with the LDA results from Refs. 15 and 59. This means that the energy difference between two particular structures, for example, agree within 10 meV/Å^2. Also, the energetical ordering of the structures are exactly the same as in Refs. 15 and 59.

From Fig. 6(a), we see that under more Ga-rich conditions the Ga adatom at the *hcp* position is the most stable structure. Under extreme Ga-rich conditions ($\mu_N=-1.25$ eV) a structure consisting of a double layer on the top of the Ga-terminated surface (contracted Ga bilayer) is the energetically favorable structure, in agreement with the theoretical results reported by Northrup *et al.*,[15] who suggested that this structure might be the one observed experimentally under such growth conditions.[10,11,16]

Under Ga-rich conditions the description using PBE is fully compatible with the LDA calculations, as we can see from Fig. 6(b), the sequence of structures is identical in LDA and PBE. Under N-rich conditions, however, LDA and PBE give qualitatively different results. While LDA predicts the N-adatom structure (on the *fcc* site) to be energetically most favorable, PBE predicts the Ga adatom (on the *hcp* site) to be energetically preferred.

A closer look at Fig. 6 shows that the discrepancy between LDA and PBE is mainly due to the formation enthalpy, which defines the width of the phase diagram (the allowed range of chemical potentials). As we have shown above, the GaN formation enthalpy in PBE is significantly underestimated (−0.64 eV compared to experimental value of −1.15 eV).

This deficiency can be largely corrected if we use the experimental GaN formation enthalpy (rather than the PBE value). The allowed range extends then into the gray region in Fig. 6(b). Applying this shift the LDA results are reproduced. In this sense, our results show that the only deficiency in PBE is the wrong description of the boundary (i.e., the binding energy of the N_2 molecule) under N-rich conditions.

3. Electronic properties

Let us first focus on the clean Ga-terminated surface [see Fig. 4(c)]. Simple electron counting arguments show that this surface has one Ga dangling bond in the top layer, which is partially filled with 7/4 of an electron. The existence of a partially filled state means that this state gives rise to a metallic surface with the Fermi energy crossing the surface

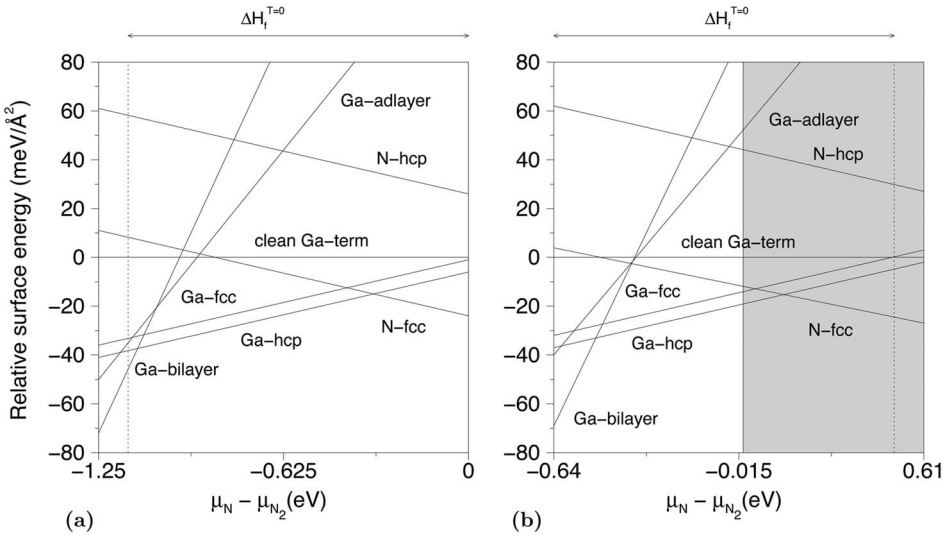

FIG. 6. Relative surface energy per angstrom squared for clean GaN (0001) surfaces as a function of the N chemical potential μ_N. (a) Using LDA and (b) using PBE. The labels have the following meaning: clean Ga term refers to the clean Ga-terminated surface, N *fcc*(*hcp*) refers to a structure with a N adatom on the *fcc*(*hcp*) site of the clean Ga-terminated surface, Ga-fcc(hcp) refers to the a structure with a Ga adatom on the *fcc*(*hcp*) site of the clean Ga-terminated surface, Ga adlayer refers to the contracted Ga-adlayer surface and Ga bilayer refers to the contracted Ga-bilayer surface (see Figs. 4 and 5). The energy zero is set to the clean Ga-terminated GaN surface. The surface area of the (1×1) unit cell is 8.84 Å^2 for LDA and 9.16 Å^2 for PBE. The experimental formation enthalpy of GaN ($\Delta H_f^{T=0}$) is indicated. The shaded region indicates the extrapolation to the experimental value of the theoretical PBE value of the formation enthalpy.

state. In Figs. 7(a) and 7(b) we show the calculated surface band structures.

In Fig. 7(a) the calculated band structure using LDA and an optimized geometry (with respect to the lattice constant) is shown. Figure 7(b) shows the equivalent result but using PBE. We can see that both exchange-correlation potentials give an almost identical dispersion for the surface state. Also, the position of the surface state above the top of the valence band of the projected bulk GaN band structure is the same for both calculations.

The main difference is that the band gap using LDA (1.7 eV) and PBE (1.4 eV) differs by 0.3 eV. The difference between LDA and PBE results may have two origins: (i) electronic effects and (ii) structural effects, since PBE leads typically to slightly larger bond lengths. To separate the two contributions we performed also a calculation within PBE but taking the geometry as optimized for LDA. Comparing this calculation with the fully optimized LDA allows us to eliminate structural effects. As can be seen in Fig. 7(a) the differences are smaller than 0.01 eV. We can therefore conclude that the differences (solid versus dotted line) in the electronic structure are primarily due to the effect of the exchange-correlation potential on the atomic structure.

Now we want to analyze the band structure of the clean Ga-terminated, Ga-adatom, contracted Ga-adlayer, and contracted Ga-bilayer surfaces. Figures 8(a)–8(d) show the band structure of these surfaces. For the clean Ga-terminated surface, as we already mentioned, there is one partially occupied surface state in the band gap due to the Ga dangling bond. This result is in good agreement with what is found in Ref. 21. The Ga-adatom structure has four surface states in the band gap, as we can see in Fig. 8(b). The two empty states are due to the two empty Ga-dangling bonds at the surface. The two occupied states are due to the three back bonds of the Ga atoms in the first layer.

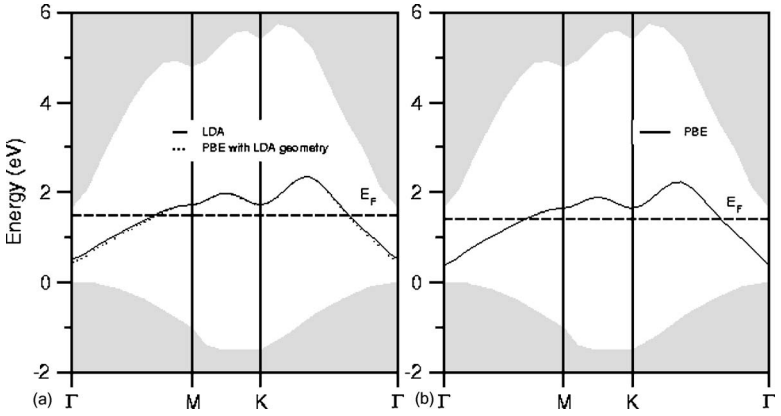

FIG. 7. Band structure of the clean (unreconstructed) GaN (0001) Ga-terminated surface using (a) LDA (solid line) and PBE with LDA optimized geometry (dotted line). (b) Shows the band structure using PBE calculation where the atomic geometry has been optimized using PBE. The dashed lines indicate the position of the Fermi level E_F. The shaded region represents the projected GaN bulk band structure.

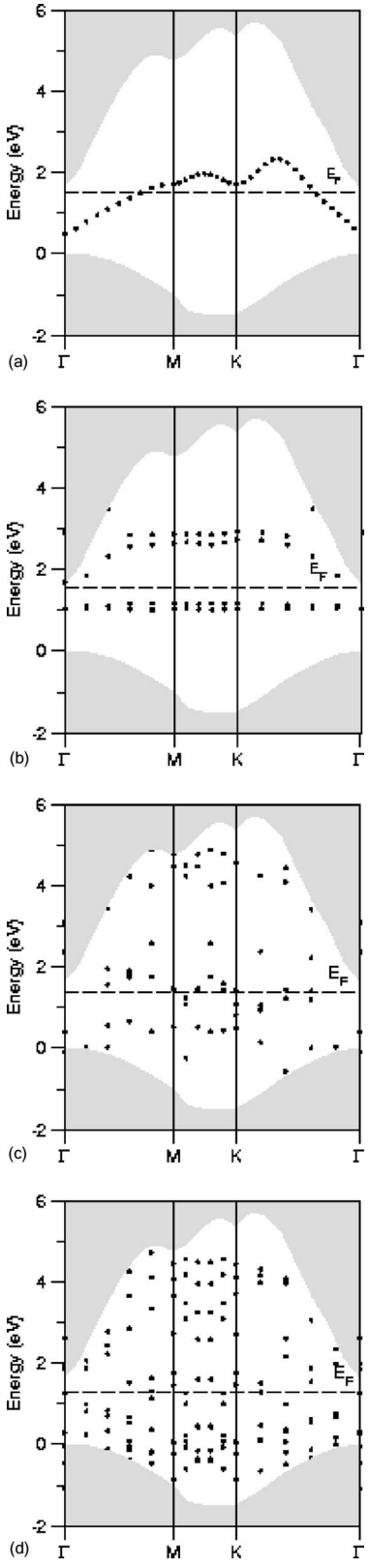

FIG. 8. Band structure of the (a) clean Ga-terminated surface, (b) Ga-adatom, (c) contracted Ga-adlayer, and (d) contracted Ga-bilayer structures. The shaded region shows the projected GaN bulk band structure. The surface states are the black dotted points. The dashed line indicates the Fermi level.

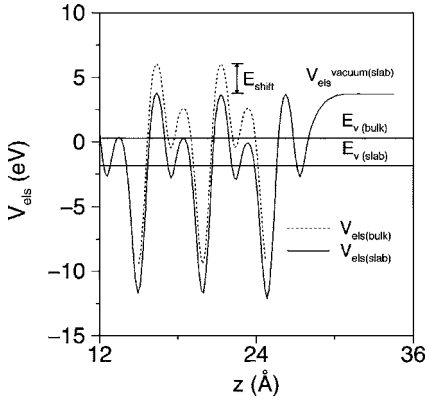

FIG. 9. Averaged electrostatic potential for the clean surface and GaN-bulk parallel to the surface normal. $E_{v(bulk)}$ is the top of the valence band in the bulk, V_{els}^{vacuum} is the electrostatic potential in the vacuum region, and E_{shift} is the shift of the top of the valence band in the slab with respect to the bulk. $E_{v(slab)}$ is the calculated top of the valence band in the slab.

The contracted Ga-adlayer and Ga-bilayer structures have metallic character, as we can see in Figs. 8(c) and 8(d). The surface states are due to the Ga adlayers. From these band structures we can see that the metallization of the surface increases with increasing Ga coverage, as expected.

In an attempt of comparison with experiment, we recall that Dhesi *et al.*[18] observed a dispersionless surface state band near the valence maximum along the Γ-*K* direction. Looking at our band structures we see that the only structures that shows dispersionless surface state close to the top of the valence band and along the Γ-*K* direction is the Ga-adatom structure.

4. Ionization energy, electron affinity and work function

So far, detailed experimental investigations of electronic properties such as ionization energy, electron affinity, and work function with respect to surface reconstructions, termination, stoichiometry, impurities, and dopants for the investigated surfaces are missing. Thus we believe our results can provide some trends on how these properties change with the surface stoichiometry.

In the following we use a procedure described in Ref. 57 to calculate the work function, electron affinity, and ionization energy. We start with the definition of these quantities. The main idea is to combine bulk and slab calculations. In the bulk calculation, the top of the valence band E_v^{bulk} is fixed relative to the bulk potential V_{els}^{bulk}.

The slab calculation determines the bulk potential relative to the vacuum level. Once the slab is sufficiently thick that both vacuum and bulk regions are well described, the electrostatic potential for the central bulklike layer in the slab $V_{els}^{slab(bulk)}$ is identical to the potential in the bulk calculation except by a constant shift (see Fig. 9). Using the results of the bulk calculation, which fixes the band energies relative to the bulk potential, we chose the potential so that the calculated top of the bulk valence band is at the energy zero.

The ionization energy is the energy difference between the vacuum level and the valence band maximum, i.e., it is the minimum energy which is necessary to lift one electron from the highest occupied state to the vacuum level. Based on it, the ionization energy is calculated as

$$I = V_{\text{els}}^{\text{vacuum}} - E_{\text{v(bulk)}} - E_{\text{shift}} = V_{\text{els}}^{\text{vacuum}} - E_{\text{v(slab)}}, \qquad (7)$$

where $V_{\text{els}}^{\text{vacuum}}$ is the electrostatic potential in the vacuum region, $E_{\text{v(bulk)}}$ is the energy of the top of the valence band in the bulk, $E_{\text{v(slab)}}$ is the energy of the top of the valence band in the slab, and $E_{\text{shift}} = V_{\text{els}}^{\text{slab(bulkregion)}} - V_{\text{els}}^{\text{bulk}}$ is the difference between the electrostatic potential in the slab in the bulk region and the electrostatic potential of the bulk. A schematic picture of this procedure for the ionization energy is shown in Fig. 9.

For metals, the energy difference between the vacuum level and the Fermi level is defined as the work function. The work function of a metal is attributed to the atomic binding energies and the surface dipole.[60] In the simplest sense, the surface dipole is a quantum mechanical effect that is attributed to the fact that the wave function of the electrons extends beyond the positive ion background. This results in excess negative charge at the surface. Just below this excess negative charge will be an unbalanced positive charge due to the ion background. The two charge sheets will form a dipole at the surface. For a semiconductor the same process may be involved, but the directional bonding at the surface can lead to even larger effects (surface reconstructions and adsorbate layers, for instance). For example, filled dangling bond type surface states will contribute with a negative charge at the surface which is balanced by a positive charge nearby. The work function is defined as

$$\phi = V_{\text{els}}^{\text{vacuum}} - E_{\text{F}}, \qquad (8)$$

where E_{F} is the Fermi level. The electron affinity relates the vacuum level to the conduction band minimum at the surface being calculated as

$$\chi = I - E_{\text{gap}}, \qquad (9)$$

where E_{gap} is the bulk band gap.

We have calculated I, ϕ, and χ for the clean Ga- and N-terminated, Ga-adatom, Ga-adlayer (contracted and noncontracted), and Ga-bilayer (contracted and noncontracted) surfaces. In Fig. 10 we show the ionization energy I as a function of the Ga coverage. The clean N terminated has 0 ML Ga coverage and the Ga terminated surface has 1 ML Ga. We can see that I changes quite significantly as the Ga coverage goes from zero (clean N-terminated surface) to 1 ML (clean Ga-terminated surface), reflecting the general instability of N-terminated surfaces.[10–12] For Ga coverages between 1 ML (clean Ga terminated) and 3.75 ML (Ga-contracted bilayer) the dependence of the ionization energy with the coverage becomes smoother, finally reaching the value of 4.12, very close to the experimental value for the work function of metallic Ga, 4.2 eV (Ref. 61) (shown in dashed line). As a matter of completeness, we have also included the values for the noncontracted Ga-adlayer and Ga-bilayer surfaces. We can see that these structures lie off the trend line, confirming the thermodynamically instability of these surfaces.[15]

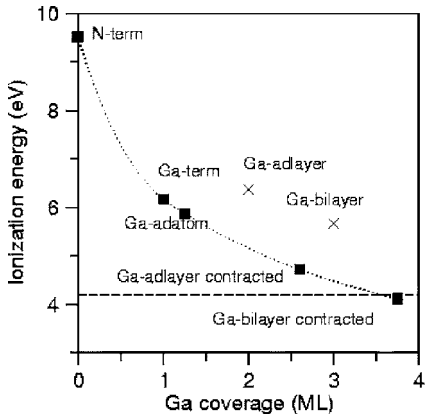

FIG. 10. Calculated ionization energy as a function of the Ga coverage for the clean GaN (0001) surfaces shown in Figs. 5, 4, and 5. The dotted line is a guide for the eyes. The crosses indicate the thermodynamically not stable structures Ga adlayer and Ga bilayer and the dashed line the work function for Ga bulk.

One of the major problems in determining theoretically the ionization energy and electron affinity is that DFT-LDA/GGA does not provide the correct band gap. Grossner *et al.*[27] included quasiparticle corrections for the top of the valence band ΔE_{v} (for the ionization energy) and the minimum of the conduction band ΔE_{c} (for the electron affinity) to correct the GaN bulk (zinc-blende structure) band gap. As the band gap of both zinc-blende and wurtzite GaN are very similar, we use quasiparticle corrections given in Ref. 27 to correct our LDA band gap of 1.7 eV. In this way, we obtain a band gap of 2.9 eV, which is closer to the experimental value of 3.4 eV. With those values we recalculated the properties listed in Table VI (values in brackets), so we can compare our values with the values in Ref. 27.

In Table VI our values for I, ϕ, and χ along with other calculations and experimental values are shown. Grossner *et al.*[27] have performed first-principles calculations of these properties for the (111) surface of zinc-blende GaN. Since the [111] direction corresponds to the $\{c\}$ axis in the wurtzite structure parallel to the hexagonal [0001] direction, we can directly compare our results with the ones in Ref. 27. In order to compare alike structures, we should compare our clean N-terminated, clean Ga-terminated, noncontracted Ga-adlayer and noncontracted Ga-bilayer surfaces with the following structures of Ref. 27: clean N-terminated, clean Ga-terminated, surface with 1 ML Ga and surface with 2 ML Ga, respectively.

For the clean N-terminated and Ga-terminated surfaces we obtain χ equal to 7.38 and 4.03 eV, while Ref. 27 reports 4.64 and 2.49 eV. For I we obtain 10.26 and 6.91 eV, while Ref. 27 gives 7.74 and 5.59 eV. Although our values are very different from the ones in Ref. 27, we can see that both quantities decrease drastically as we change the Ga coverage from 0 (clean N terminated) to 1 ML (clean Ga terminated). For higher Ga coverages we obtain for χ 4.23 (Ga-adlayer noncontracted) and 3.53 eV (Ga-bilayer noncontracted) and

TABLE VI. Calculated and experimental values for the electron affinity χ, work function ϕ, and ionization energy I for the clean GaN (0001) surfaces shown in Figs. 4(b), 4(c), 4(e), and 5(a)–5(d). The values in brackets are calculated using the quasiparticle corrections for the valence band maximum (−0.74 eV) and conduction band minimum (0.44 eV) from Ref. 27.

Reference theory	Surface	χ (eV)	ϕ (eV)	I (eV)
This work	(0001) clean N-terminated	7.82 (7.38)	9.06	9.52 (10.26)
This work	(0001) clean Ga-terminated	4.47 (4.03)	4.42	6.17 (6.91)
This work	(0001) Ga-adatom hcp	4.17 (3.73)	4.20	5.87 (6.61)
This work	(0001) Ga-adlayer(non-contracted)	4.67 (4.23)	5.31	6.37 (7.11)
This work	(0001) Ga-adlayer(contracted)	3.20 (2.76)	3.40	4.72 (5.46)
This work	(0001) Ga-bilayer(non-contracted)	3.97 (3.53)	4.80	5.67 (6.41)
This work	(0001) Ga-bilayer(contracted)	2.42 (1.98)	3.10	4.12 (4.86)
27	(111) clean N-terminated	4.64		7.74
27	(111) clean Ga-terminated	2.49		5.59
27	(111) with 1 ML Ga	1.79		4.89
27	(111) with 2 ML Ga	2.02		5.12
27	(111) with 3 ML Ga	1.78		4.88
69	(0001) clean		4.5	
Exp.				
25	(0001) *n*-type	3.50±0.10	4.30±0.10	6.90
25	(0001) *p*-type	3.50±0.10	5.90±0.10	6.90
62	*n*-type	4.10		
62	intrinsic	2.10		
27				6.80
23		3.10±0.20		
63	*n*-type		3.88	
64	Ga-face			
65			4.30±0.15	
24		3.2		
26	(0001) *p*-type	2.6±0.1		
26	(0001) *n*-type	2.8±0.1		
61	Ga-bulk		4.20	

for I 7.11 (Ga-adlayer noncontracted) and 6.41 eV (Ga-bilayer noncontracted), i.e., the electronic properties decrease as the Ga-coverage increases. On the other hand, Ref. 27 obtains χ 1.79 (Ga 1 ML) and 2.02 eV (Ga 2 ML) and for I 4.89 (Ga 1 ML) and 5.12 eV (Ga 2 ML) and no trend is found in this case.

Compared to experimental values, we can see from Table VI that the best agreement for our structures is obtained between the clean Ga-terminated surface and the (0001) *n*-type surface reported in Ref. 25.

IV. CONCLUSIONS

We have performed density-functional theory calculations for the N_2 molecule, GaN-bulk, Ga-bulk, and GaN (0001) surfaces. Regarding the bulk phases, PBE does not lead to real improvement for the structural properties, since LDA always underestimates the experimental values, while PBE overestimates them by the same amount. In general, PBE performs better in describing the binding energy of solids and molecules. The formation enthalpy of GaN using PBE is strongly underestimated, while LDA provides a value very close to the experiment.

We have found a very good qualitative agreement between LDA and PBE for the band structure. We conclude that the difference in the band gap is attributed only to different descriptions of the lattice parameters. Furthermore, we have shown that LDA and PBE give very similar results for the atomic relaxations and electronic structure of the GaN (0001) surfaces. We concluded that PBE does not provide the same energetic ordering of structures, but that this is due to the underestimation of the GaN formation enthalpy, which is a well-known problem for all class of nitrides. If the formation enthalpy is corrected to the experimental value, the correct ordering is reproduced. Also, our results clearly showed that the position of the surfaces states is not affected by the choice of the exchange-correlation functional.

Our results of the ionization energy, electron affinity and work function show a good agreement with a *n*-type GaN (0001) surface,[24] although a comparison with experimental data is not straightforward. This mainly stems from the difficulty in determining experimentally the stoichiometry and termination of the surfaces.

*Corresponding author. Electronic mail: andreia.luisa@fysik.uu.se

[1] S. Nakamura, T. Mukai, and M. Senoh, Appl. Phys. Lett. **64**, 1687 (1994).
[2] S. Nakamura, M. Senoh, S. Nagahama, N. Iwasa, T. Yamada, T. Matsushita, H. Kiyoku, and Y. Sugimoto, Jpn. J. Appl. Phys., Part 2 **35**, L74 (1996).
[3] S. Nakamura and G. Fasol, *The Blue Laser Diode* (Springer-Verlag, Berlin, 1997).
[4] G. Mula, C. Adelmann, S. Moehl, J. Oullier, and B. Daudin, Phys. Rev. B **64**, 195406 (2001).
[5] B. Heying, R. Averbeck, L. F. Chen, E. Haus, H. Riechert, and J. S. Speck, J. Appl. Phys. **88**, 1855 (2000).
[6] L. X. Zheng, M. H. Xie, S. M. Seutter, S. H. Cheung, and S. Y. Tong, Phys. Rev. Lett. **85**, 2352 (2000).
[7] C. Adelmann, J. Brault, G. Mula, B. Daudin, L. Lymperakis, and J. Neugebauer, Phys. Rev. B **67**, 165419 (2003).
[8] G. Koblmüller, R. Averbeck, H. Riechert, and P. Pongratz, Phys. Rev. B **69**, 035325 (2004).
[9] O. Ambacher, J. Phys. D **31**, 2653 (1998).
[10] H. Chen, R. M. Feenstra, J. E. Northrup, T. Zywietz, J. Neugebauer, and D. M. Greve, J. Vac. Sci. Technol. B **18**, 2284 (2000).
[11] A. R. Smith, R. M. Feenstra, D. W. Greve, M.-S. Shin, M. Skowronski, J. Neugebauer, and J. E. Northrup, J. Vac. Sci. Technol. B **16**, 2242 (1998).
[12] A. R. Smith, R. M. Feenstra, D. W. Greve, M. S. M.-S. Shin, J. Neugebauer, and J. E. Northrup, Surf. Sci. **423**, 70 (1999).
[13] F. Widmann, B. Daudin, G. Feuillet, Y. Samson, J. L. Rouvière, and N. Pelekanos, Appl. Phys. Lett. **83**, 7618 (1998).
[14] F. Widmann, B. Daudin, G. Feuillet, N. Pelekanos, and J. L. Rouvière, Appl. Phys. Lett. **73**, 2642 (1998).
[15] J. E. Northrup, J. Neugebauer, R. M. Feenstra, and A. R. Smith, Phys. Rev. B **61**, 9932 (2000).
[16] M. M. Sung, J. Ahn, V. Bykov, J. W. Rabalais, D. D. Koleske, and A. E. Wickenden, Phys. Rev. B **54**, 14652 (1996).
[17] Z. X. Yu, S. Y. Tong, S. Xu, S. Ma, and H. Wu, Surf. Rev. Lett. **10**, 831 (2003).
[18] S. S. Dhesi, C. B. Stagarescu, K. E. Smith, D. Doppalapudi, R. Singh, and T. D. Moustakas, Phys. Rev. B **56**, 10271 (1997).
[19] Y.-C. Chao, C. B. Stagarescu, J. E. Downes, P. Ryan, K. E. Smith, D. Hanser, M. D. Bremser, and R. F. Davis, Phys. Rev. B **59**, R15586 (1999).
[20] S. M. Widstrand, K. O. Magnusson, L. S. O. Johansson, and M. Oshima, Surf. Sci. **584**, 169 (2005).
[21] F. H. Wang, P. Krüger, and J. Pollmann, Phys. Rev. B **64**, 035305 (2001).
[22] V. Timon, S. Brand, S. J. Clark, M. C. Gibson, and R. A. Abraham, Phys. Rev. B **72**, 035327 (2005).
[23] S. P. Grabowski, M. Schneider, H. Nienhaus, W. Mönch, R. Dimitrov, O. Ambacher, and M. Stutzmann, Appl. Phys. Lett. **78**, 2503 (2001).
[24] V. M. Bermudez, J. Appl. Phys. **80**, 1190 (1996).
[25] C. I. Wu, A. Kahn, N. Taskar, D. Dorman, and D. Gallagher, J. Appl. Phys. **83**, 4249 (1998).
[26] K. M. Tracy, W. J. Mecouch, R. F. Davis, and R. J. Nemanich, J. Appl. Phys. **94**, 3136 (2003).
[27] U. Grossner, J. Furthmüller, and F. Bechstedt, Phys. Status Solidi B **216**, 675 (1999).
[28] P. Hohenberg and W. Kohn, Phys. Rev. **136**, B864 (1964).
[29] W. Kohn and L. J. Sham, Phys. Rev. **140**, A1133 (1965).
[30] D. M. Ceperley and B. J. Alder, Phys. Rev. Lett. **45**, 566 (1980).
[31] J. P. Perdew and A. Zunger, Phys. Rev. B **23**, 5048 (1981).
[32] J. P. Perdew, K. Burke, and M. Ernzerhof, Phys. Rev. Lett. **77**, 3865 (1996).
[33] N. Troullier and J. L. Martins, Phys. Rev. B **43**, 1993 (1991).
[34] N. Troullier and J. L. Martins, Phys. Rev. B **43**, 8861 (1991).
[35] H. J. Monkhorst and J. D. Pack, Phys. Rev. B **13**, 5188 (1976).
[36] L. Bosio, J. Chem. Phys. **68**, 1221 (1978).
[37] R. W. G. Wyckoff, *Crystal Structures* (Wiley, New York, 1962), Vol. 1, p. 22.
[38] L. Bosio, A. Defrain, H. Curien, and A. Rimsky, Acta Crystallogr., Sect. B: Struct. Crystallogr. Cryst. Chem. **25**, 995 (1969).
[39] L. Bosio, H. Curien, M. Dupont, and A. Rimsky, Acta Crystallogr., Sect. B: Struct. Crystallogr. Cryst. Chem. **28**, 1974 (1972).
[40] L. Bosio, H. Curien, M. Dupont, and A. Rimsky, Acta Crystallogr., Sect. B: Struct. Crystallogr. Cryst. Chem. **29**, 367 (1973).
[41] M. Bernasconi, G. L. Chiarotti, and E. Tosatti, Phys. Rev. B **52**, 9988 (1995).
[42] M. Fuchs, J. L. F. DaSilva, C. Stampfl, J. Neugebauer, and M. Scheffler, Phys. Rev. B **65**, 245212 (2002).
[43] M. Fuchs, M. Bockstedte, E. Pehlke, and M. Scheffler, Phys. Rev. B **57**, 2134 (1998).
[44] S. Strite and H. Morkoç, J. Vac. Sci. Technol. B **10**, 1237 (1992).
[45] C. Stampfl and C. G. VandeWalle, Phys. Rev. B **59**, 5521 (1999).
[46] K. Karch, J.-M. Wagner, and F. Bechstedt, Phys. Rev. B **57**, 7043 (1998).
[47] C. Y. Yeh, Z. W. Lu, S. Froyen, and A. Zunger, Phys. Rev. B **46**, 10086 (1992).
[48] J. H. Edgar, ed., *Properties of Group-III Nitrides and EMIS Data Reviews* (IEE, London, 1994).
[49] X. J. Kong, C. T. Chan, K. M. Ho, and Y. Y. Ye, Phys. Rev. B **42**, 9357 (1990).
[50] M. Körling and J. Häglund, Phys. Rev. B **45**, 13293 (1992).
[51] P. H. T. Philipsen and E. J. Baerends, Phys. Rev. B **54**, 5326 (1996).
[52] I. H. Lee and R. M. Martin, Phys. Rev. B **56**, 7197 (1997).
[53] A. Zoroddu, F. Bernardini, P. Ruggerone, and V. Fiorentini, Phys. Rev. B **64**, 045208 (2001).
[54] T. K. Zywietz, Thermodynamische und kinetische Eigenschaften von Galliumnitrid-Oberflächen, Ph.D. thesis, Weissensee Verlag, Berlin, 2000.
[55] T. Zywietz, J. Neugebauer, and M. Scheffler, Appl. Phys. Lett. **73**, 487 (1998).
[56] K. Rapcewicz, M. Buongiorno-Nardelli, and J. Bernholc, Phys.

Rev. B **56**, R12725 (1997).
[57] G.-X. Qian, R. M. Martin, and D. J. Chadi, Phys. Rev. B **38**, 7649 (1988).
[58] A. Kley, Theoretische Untersuchungen zur Adatomdiffusion auf niederindizierten Oberflächen von GaAs, Ph.D. thesis, TU, 1997.
[59] C. Bungaro, K. Rapcewicz, and J. Bernholc, Phys. Rev. B **59**, 9771 (1999).
[60] A. Zangwill, *Physics at Surfaces* (Cambridge University Press, Cambridge, 1988).
[61] V. S. Fomenko, *Emissionye Svoistva Materialov* (Izd. Naukova Dumka, Kiev, 1981).
[62] J. I. Pankove and H. Schade, Appl. Phys. Lett. **25**, 53 (1974).
[63] M. Eyckeler, W. Mönch, T. U. Kampen, R. Dimitrov, O. Ambacher, and M. Stutzman, J. Vac. Sci. Technol. B **16**, 2224 (1998).
[64] G. Koley and M. G. Spencer, J. Appl. Phys. **90**, 337 (2001).
[65] T. Valla, P. D. Johnson, S. S. Dhesi, K. E. Smith, D. Doppalapudi, T. D. Moustakas, and E. L. Shirley, Phys. Rev. B **59**, 5003 (1999).
[66] C. Kittel, *Introduction to Solid State Physics* (Wiley, New York, 1996).
[67] *Handbook of Physics and Chemistry*, edited by D. R. Lide (CRC Press, New York, 1995).
[68] R. C. Powell, N. E. Lee, Y. W. Kim, and J. E. Greene, J. Appl. Phys. **73**, 189 (1993).
[69] M. H. Tsai, O. F. Sankey, K. E. Schmidt, and I. S. Tsong, Mater. Sci. Eng., B **88**, 40 (2002).